SCIENCE SET
OPEN ACCESS PUBLISHERS

Research Article

World Journal of Sensors Network Research

Synthesis and Characterization of 2D Graphene Thin Films for Optoelectronic Gadgets

Ladan, H.M. A[1*]., Adamu, A. S[2]., Buba, A.D. A[3]., & Umar A[4]

[1]*Department of Physics, Faculty of Science, Sa'adu Zungur University, Bauchi State, Nigeria*
[2]*Department of Electrical Engineering, Ahmadu Bello University, Zaria, Nigeria*
[3]*Department of Physics, Faculty of Science, University of Abuja, Abuja*
[4]*Department of Chemistry, Faculty of Science, University of Abuja, Abuja, Nigeria*

[*]**Corresponding author:** Ladan HMA, Department of Physics, Faculty of Science, Sa'adu Zungur University, Bauchi State, Nigeria.

Submitted: 30 November 2024 **Accepted:** 06 December 2024 **Published:** 15 January 2025

Citation: *Ladan, H. M. A., Adamu, A. S., Buba, A. D. A., & Umar, A. (2025). Design of high-performance graphene lead-free perovskite solar cells by numerical modeling based on coupled differential equations. Wor Jour of Sens Net Res, 2(1), 01-07*

Abstract

This investigation has shown for the first time, the possibility of obtaining high quality 2D graphene thin films for optoelectronic gadgets from the abundant graphite in Nigeria. In the study, synthesis and characterization of graphene from natural graphite and the determination of the electrical conductivity of the thin films were conducted. The samples were characterized by X-ray diffraction (XRD), X-ray fluorescence (XRF), field emission scanning electron microscopy and energy dispersive X-ray (FESEM and EDX) to show their structural and compositional features. XRF study showed the mineral compositions as MgO (4.35%), SiO2 (25.14%), SrO (9.73%), CdO (1.99%) and C (15%). XRD pattern indicated perfectly crystallized graphene flakes. Surface morphology by SEM analysis revealed closely packed, layered and spongy structures. EDX studies indicated the elemental composition as Carbon (86.34%), Molybdenum (10.37%), Potassium (2.38%) and Titanium (0.91%). The reduced graphene oxide (RGO)-TiO2 composite thin films displayed glistering surfaces due to the less density of electronic trap states and improved absorption in UV-visible region making them suitable for optoelectronic devices. The resistivity of 1.9592, 12.9366, 2.5419 and 25.1256 s/m were recorded for GO, RGO, GO-TiO2 and RGO-TiO2 thin films. The study has revealed that graphite and its products (GO/RGO) are of high quality. They can be produced for academic research and industrial integration at a lower cost compared to the imported types without detailed characterization systems into African market.

Keywords: Graphene Oxide, Graphene Flakes, Graphene-TiO2, Graphite, Electrical Conductivity, FESEM, EDX, XRF

Introduction

Graphite is a carbon-based material and are available in abundant especially in Kaduna, Adamawa, Niger, Taraba, Kogi and Bauchi state of Nigeria. The graphite ore is mixed with clay and other metallic impurities. It can be purified by froth floatation in order to concentrate the mineral value in the ore using hydrocarbons [3, 3]. Graphene is a two-dimensional allotrope of carbon in a hexagonal pattern. It is very strong and has a high tensile strength. Graphene oxide (GO) can be synthesized by oxidizing graphite using the Hummer's method. It has carboxylic, epoxide, alcohol, and carbonyls groups at the base and surfaces. The thermal reduction system can be employed to produce the reduced GO. Graphene has attracted huge research interest due to their high charge mobility, conductivity, transparency, flexibility and mechanical strength [4]. Geim et al. won the 2010 Nobel Prize for their work on graphene. It has wide areas of applications especially in Agriculture, photo-catalysis, nanotechnology, medical and pharmaceutical research, energy storage and conversion systems among others [6, 7].

In 1859, the first production of oxidized graphite was reported by Brodie using potassium chlorate in fuming HNO3 [8]. Staudenmaier used fuming HNO3 and introduced concentrated H2SO4 followed by the gradual addition of the chlorate as the oxidizing agent [9]. In 1958, Hummers' method was introduced and is widely used today by treating the graphite with NaNO3 and

KMnO4 in concentrated H2SO4 improved Hummers' technique by introducing phosphoric acid to produce GO [10, 11]. Single graphene nanosheets were first reported in 2004 by mechanical exfoliation (scotch tape) using epitaxial chemical vapor deposition (CVD) of the layered graphite [12]. Graphene-titanium dioxide (TiO2) composite improves the conductivity, mobility and absorptivity in the UV visible region due to high density of electronic trap states, low carrier mobility and electronic conductivity [13, 14].

Optoelectronics is employed in the design and production of gadget such as solar cells, photodetectors, light semiconducting emitting diodes (LEDs), photodiode, emitters and sensors for communications, automation system, LASERs and phototransistors. Their sensitivities to UV visible light are essential for efficient uses [15]. The application of GO-TiO2 as carrier transporter enhances the efficiency of the device due to reduction in density of electronic trap states, increase in carrier mobility, and conductivity. Graphite has not been explored due to the focus on petroleum as a source of revenue generation.

There is need for the synthesis and characterization of high-quality graphene from NG that are available in abundant in almost all the states of the federation. In this study, synthesis and characterization of graphene and graphene-TiO2 thin films were conducted using NG. The characterization of the samples was conducted using X-ray fluorescence and diffraction (XRF/XRD) analysis, field emission scanning electron microscopy (FESEM) and energy dispersive x-ray (EDX). The available graphite if processed in large quantities can be exported to Korea, Europe, China, USA, and south East Asia for industrial production. It can also be a substitute to the highly expensive type imported in which detailed characterizations were not included for enhanced academic and research activities.

Experimental Procedure

Materials

The materials used for the study includes natural graphite (NG) powder (Adamawa), TiO2 (Solaronix, Switzerland), potassium permanganate (KMnO4), Sodium nitrate (NaNO3), Tetraoxosulphate (VI) acid H2SO4 (98%), purified water, Hydrogen peroxide (H2O2, 30%) and Hydrochloric acid (HCl). All the analytical grades were used without further purification. The graphite ore was obtained from Mubi in Adamawa state was beneficiated at Kaduna Polytechnic, Kaduna, Kaduna state, Nigeria to concentrate the carbon content and remove the impurities.

Methods

Synthesis of GO and Reduced GO

2 g of the NG powder, 10 ml of conc. H2SO4, and 1 g of KMnO4 were mixed together and stirred with 1.5 g of NaNO3 in a 500 ml beaker. At the temperature below 5oC, the mixture was stirred using a magnetic stirrer for half an hour. 100 ml of purified water was added gradually to form a dark brown color, with increasing temperature to 45 oC. The mixture was kept on a magnetic stirrer at 95 °C and continuous stirring was done until a bright-yellow mixture was obtained. 10 ml H2O2 (30%) was added to the solution to form a golden yellow colouration. After centrifugation at 1000 rpm for 5 minutes and separation, the purification process to remove metal ions/acid radicals were carried out using 10% HCl at pH ~7. The GO obtained was reduced by thermal method to have reduced graphene oxide (RGO).

Preparation and Characterization of TiO2:GO thin films by Spin Coating

The fluorine-doped tin oxide (FTO) transparent glass substrates (Solaronix, 7Ω/sq) were ultrasonically cleaned in acetone and distilled water. The TiO2 nanoparticles (Solaronix) and graphene sheets were mixed in a weight ratio of 10:1. The GO and RGO was exfoliated by chemical process. 1 g of each sample was poured in 100 ml volumetric flask containing ethanol (10 ml). The solution was sonicated until a homogenous (clear) mixture was obtained. The substrates were thoroughly cleaned in acetone and dried in nitrogen gas. With a spin coater, a tiny drop of each sample was spin coated at 500 rpm on FTO glass. After spin coating, the specimens were annealed at 300, 500 and 600oC (fig. 1) for the RGO (A), GO (B), RGO-TiO2 (C), and GO-TiO2 (D) based thin films (fig. 2) were further sintered in an oven at 100°C for 10 min according to Li et al., 2019

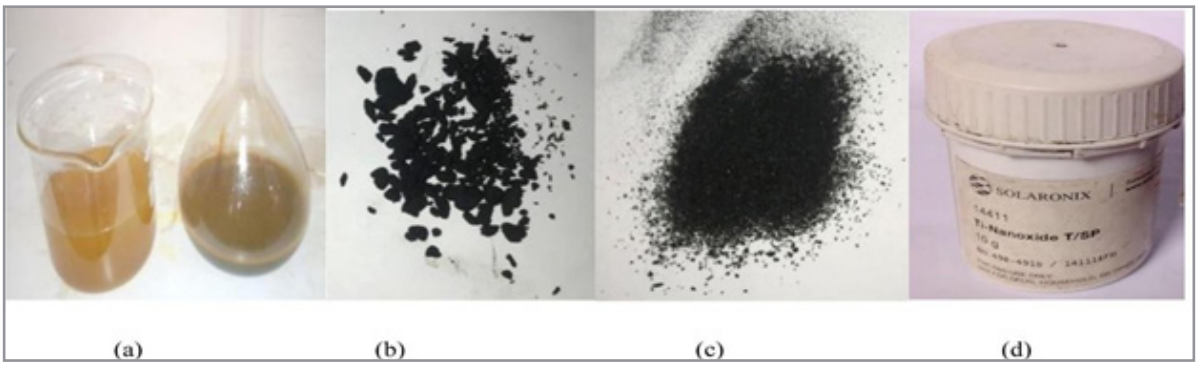

Figure 1: GO in (a) solution (b) clustered (c) powdered (d) semiconducting TiO2 (Ti-Nanoxide, T/SP)

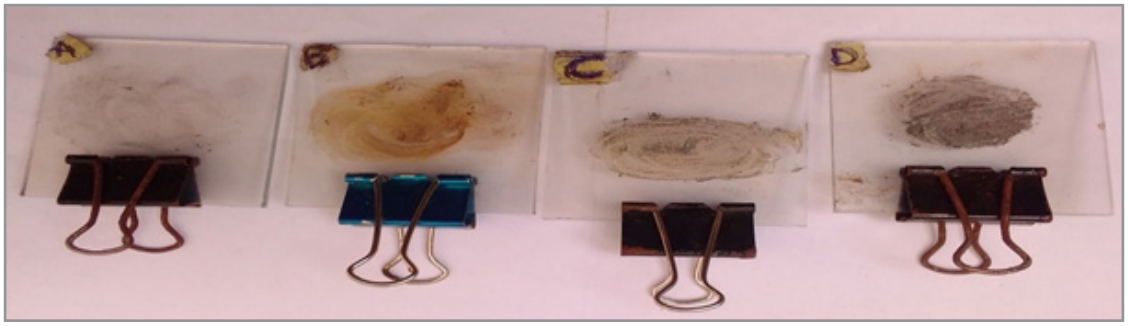

Figure 2: Graphene thin films (a) RGO (b) GO (c) TiO2-RGO (d) TiO2-GO

Characterization of the Samples

The XRF analysis of the NG was carried out on XRF (ARL QUANTX thermo fisher, UMYU Katsina) to show the chemical compositions and the fixed carbon contents (FCC). The SEM revealed the morphological features of the samples and the elemental compositions using. The morphological features of the samples were observed on SEM (PRO X, Phenonm world MVE 01570775, UMYU, Katsina) and the EDX analysis was conducted on an Amatek device (SEM AUST) to record the elemental compositions. The phase composition was identified using XRD (ARL XTRA thermo fisher) with Cu*kx* radiation (k = 1.5406 nm) at 45kV and 40 mA to show the crystalline phase of the TiO2: GO sample.

Electrical Properties of the GO and RGO

The electrical characterization of the thin films was performed using four-point probe (4200 Keithley) at room temperature. The film thickness was measured by Alpha step profilometer. The resistivity *p* of GO and RGO thin film can be expressed as

$$\rho = R_S\, t \tag{1}$$

where R_s is sheet resistance and is given by

$$R_s = \frac{\rho}{t} = \frac{\pi}{ln2}\left(\frac{V}{I}\right) = K\left(\frac{V}{I}\right) = \left(\frac{V}{I}\right)4.532 \tag{2}$$

The resistivity of a thin sheet ρ is given by:

$$\rho = \frac{\pi t}{ln2}\left(\frac{V}{I}\right) \tag{3}$$

The geometric factor K, depends on the spacing and configuration of the probes (Petersen et al., 2002; Hasegawa et al., 2006; Li et al., 2012).

Results and Discussion

XRF Analysis of the Graphite Ore

XRF analysis showed that the mineral compositions were Fe2O3, CuO, MgO, BaO, SiO2, P2O5, K2O, TiO2, CeO2, SrO and CdO. The sample has approximately fixed carbon content of 15% which is low due to the presence of other minerals and elements.

XRD Analysis of the Graphite and Graphene Oxides

XRD is a way to determine crystal structures and impurity in substances by irradiating the material with incident x- rays to determine the crystal structures, mineral phase, and identification of impurities. XRD patterns of the graphite are perfectly crystallized and closely packed [16, 17]. The XRD spectra showed a sharp diffraction peak at about 2θ = 27º at reflection plane (002) and the inter-planar spacing dhkl was calculated with the Bragg's law

$$d = \frac{\lambda}{2sin\theta} = 3.36\text{A} \tag{4}$$

where λ is the wavelength and hkl are miller indices and θ is the diffraction angle For GO and RGO, the XRD diffractogram indicated the crystal structure. The peak for both GO and RGO samples show a slight difference at 12o due to reflection plane (002) of GO and 13o for RGO. Diffraction peak at 2θ = 11.01º at reflection plane (001) confirmed formation of GO. The reduction of GO was confirmed by diffraction peak that appeared at 2θ = 26.60 (Table 1) reflection plane (002). When graphite is oxidized to GO due introduction of intercalated functional groups (epoxyl, hydroxyl, carbonyl and carboxyl), XRD peak shift from about 27o to 50o and no sharp peak appeared in the XRD result from 10o to ~27o due to incomplete oxidation of graphite [18, 19]. The RGO-TiO2 displayed a glistering surface due to less density of electronic trap states and improved absorption in the UV region making suitable for optoelectronic devices since over 80% of the UV radiation in that range can be absorbed by the applied system. The associated visible reference codes of 01-075-1537, 01-082-0511 and 96-901-2706 for TiO2, SiO2 and C6 (Table 2) corresponding to 250, 210 and 420 respectively (Figure 4 and 5).

Table 1: Peak list of RGO

Pos. [°2Th.]	Height [cts]	Left [°2Th.]	d-spacing [Å]	Rel. Int. [%]
26.6056	102.81	0.1535	3.35048	51.13
50.0467	201.05	0.0768	1.82260	100.00
67.6285	147.48	0.0936	1.38418	73.36

Table 2: Pattern list of TiO_2

Visible Ref. Code	Score	Compound Name	Scale factor	Chem. Formula
01-075-1537	25	Titanium Dioxide	1.000	TiO_2
01-082-0511	21	Silicon Oxide	0.496	SiO2
96-901-2706	42	2D (Oxidized Graphite)	0.496	C6

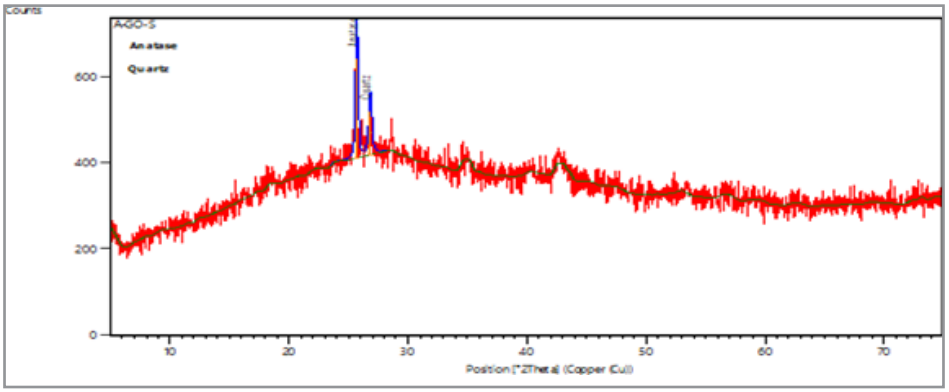

Figure 4: XRD pattern of the TiO2 on quartz substrate

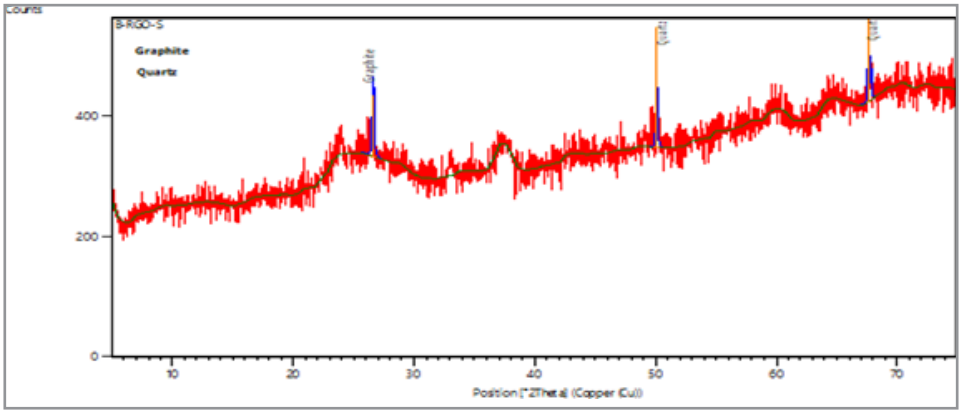

Figure 5: XRD pattern of the RGO on quartz

SEM and EDX Analysis of the Graphite, GO and RGO

SEM analysis at magnification of 500 and 1000x and working distance of 1.07 mm revealed the morphological characteristics of the graphite samples with shiny and reflective surfaces when exposed to light. The surface morphology of GO thin film revealed a porous spongy structure with the graphene sheet not well connected together, a hexagonal surface in layers. This shows that graphite has been exfoliated during the oxidation process. It can be attributed to the distorted graphene sheets when oxygen and other functional groups attached to the carbon atoms. GO sample looks clustered (Figure 6).

The SEM micrograph of RGO-TiO2 at magnification of 250x and 2000x displayed a glistering and reflecting surfaces in layers owing to the presence of TiO2 due to high density of electronic trap states and improve absorption in the UV region of the spectrum [20]. (Figure 6).

Energy dispersive x-ray (EDX) analysis of GO thin films on gold substrate showed peaks due to presence of carbon C (86.34%) for electrons in the K shell, Mo (10.37%) L shell, K (2.38%) K shell and Ti (0.91%) in K shell (Figure 7). While the presence of P, S, and K were due to H2SO4 and KMnO4 used as oxidizing agent, the presence of Si, Mg and Na were from the glass substrate [21, 22].

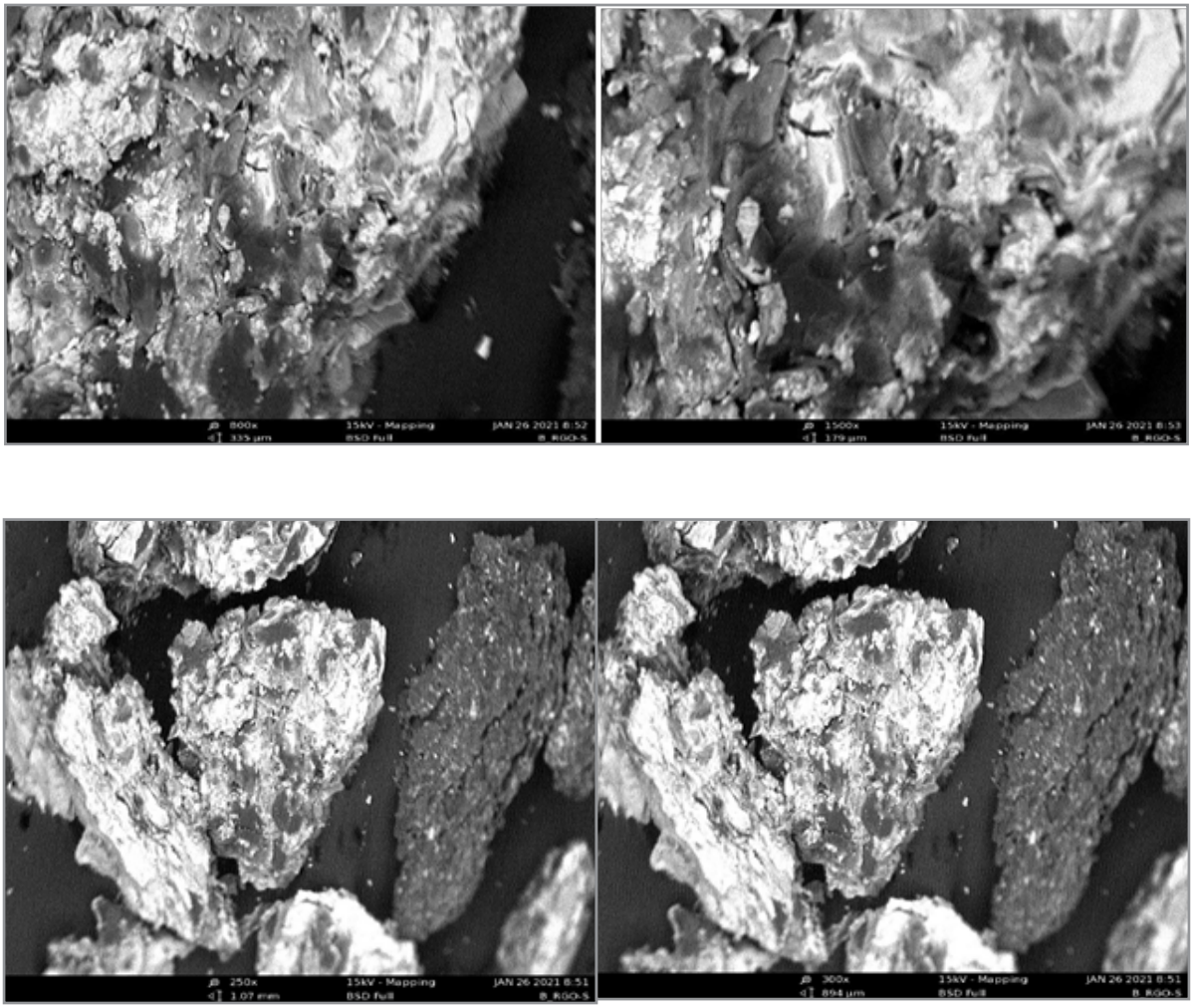

Figure 6: SEM micrograph of RGO at magnification of 800x, 1500x, 250x, 300x

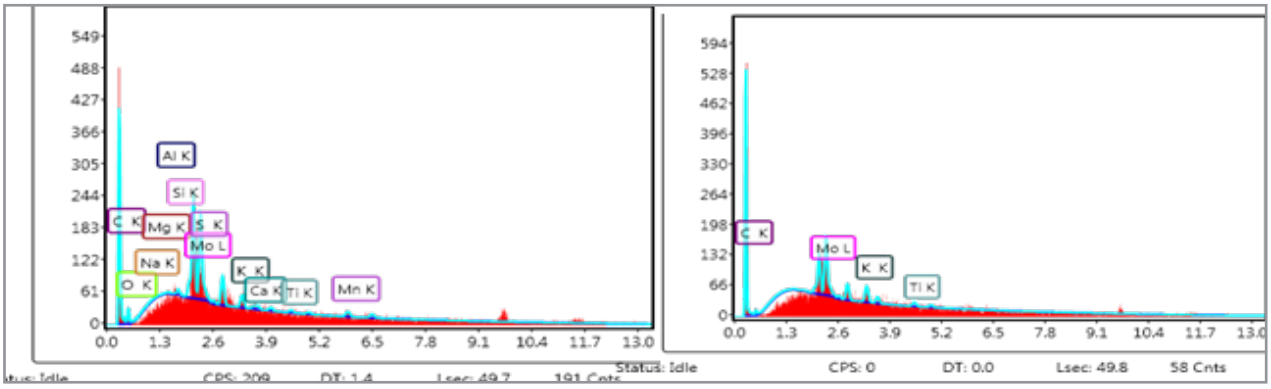

Figure 7: EDX micrograph of (a) GO (b) RGO showing the elements and the elemental counts

The Conductivity of the GO and RGO Thin Films

GO behaves like a semiconductor due to oxygenated functional groups some of the sp2-bonded carbon atoms become sp3. Since the interlayer spacing of GO compared to RGO increases due to increase in oxygen functional groups create high mesoporous volume and reduces electrical conductivity. The hydroxyl, carboxyl, carbonyl, and epoxy groups introduced to the graphite layers by oxidation process decrease the interaction between Van-der Waals forces. The presence of defects influences the electrical conduction and upon thermal reduction to RGO the conductivity drastically improved due to decrease in oxygenated functional groups. The TiO2 has low electron mobility, high density of electronic trap states and low absorption in the UV region. GO and increases the conductivity of TiO2 (Table 3). The electron transport in GO-TiO2 and RGO-TiO2 is governed by detrapping of electrons from sub-band gap states deep in the tail of the density-of-states to the conduction band (CB) in line with the multi- trapping mechanism. Trap states play a crucial

role in TiO2 the occupation of the sub-band gap states at a particular energy EA can be expressed by the Fermi-Dirac distribution function:

Where f (E) is the probability that a state of energy E is occupied, EF is the Fermi energy, K_b is the Boltzmann's constant, T is absolute temperature

$$F(E_A - E_{Fn}) = \frac{1}{1 + e^{(E_A - E_{Fn})/K_b T}} \quad (5)$$

Where f (E) is the probability that a state of energy E is occupied, EF is the Fermi energy, K_b is the Boltzmann's constant, T is absolute temperature. The density of carriers at this energy can be expressed as, nA = NAEA.

Assuming that electrons can only be transported via the CB, then density of electrons in the CB varies with the position of the quasi-Fermi level for the electrons and the conductivity of the film

$$n_{CB} = N_{CB} e^{(E_A - E_{Fn})/K_b T} \quad (6)$$

Where nCB is the density of electrons in the CB, EFn is the quasi-Fermi level for the electrons

The conductivity can also be expressed in terms of the Fermi energy, EF as

$$\sigma(E_F) = e\mu_e n_e(E_F) \quad (7)$$

Where NA is the total number of available sites at this energy, e is the electronic charge, u_e represent the electron mobility, and r_e is the electron carrier density [23].

The average electron mobility depends upon the probability of the electrons being in the CB, and conductivity increases as the quasi-Fermi level for electrons approaches the CB energy. It implies that any modification and doping that eliminates deep trap states will increase the conductivity of the samples and higher current output from the device will be achieved when applied in optical and photovoltaic cells [24, 25]. The results of the conductivity measurement for GO and RGO thin films are in Table 3 compared with similar studies in literature. The reduction in resistivity from room temperature to 5000C revealed that GO synthesized has been drastically reduced to RGO. Improvement in the electrical conductivity of the samples 1.9592, 12.9366, 2.5419 and 25.1256 Sm−1 for the (a) RGO (b) GO (c) TiO2-RGO (d) TiO2-GO thin films are indication of their suitability for applications in photovoltaic cells and energy conversion devices, the same order reported in similar studies in the literature [26]. The application of graphene films in applications such as transparent electrodes is governed by sheet resistance and visible-light transmission. Each of these criteria having its own unique requirements in improving the optoelectronic properties. Either of these properties can be fine-tuned to the desired value by changing the thickness of the graphene film. The smaller the sheet resistance, the higher the transmission of light through it.

Table 3: The conductivity of the GO and RGO thin films

Graphene	Thickness t	V(mV)	I(A) x 10^{-9}	*RS* (⁄sq) x 10^{6}	(m)	1 S/m p	References
GO-N	0.022	28.0	5.47	23.20	0.5104	1.9592	This study
RGO-N	0.015	50.0	44.01	5.15	0.0773	12.9366	This study
GO-S	0.022	14.6	3.70	17.88	0.3934	2.5419	This study
RGO-S	0.015	53.0	90.65	2.65	0.0398	25.1256	This study
GO-NGF	0.027	25.0	4.95	22.90	0.6183	1.6173	Eluyemi et al., 2016
RGO-NGF		50.0	45.69	4.95	0.1330	7.5188	
RGO	0.025	-	-	0.0179	-	23.30	Wan et al., 2012

Summary and Conclusion

In this study, a compositional analysis of Nigerian graphite, synthesis and characterization of GO and RGO by modified Hummers method were carried out. XRF study showed the presence of MgO (4.35%), SiO2 (25.14%), SrO (9.73%), CdO (1.99%) and C (15%). The XRD spectra showed a sharp diffraction peak and inter-planar spacing of 3.370Å. SEM analysis has revealed reflective surfaces in layers. The electrical measurements showed the conductivity of RGO is the highest and the resistivity of 1.9592, 12.9366, 2.5419, 25.1256 S/m for GO, RGO, GO-TiO2 and RGO-TiO2 respectively. The smaller the sheet resistance, the higher the transmission of light through it. The present study has revealed that the Nigerian natural graphite is of high quality which can be used to synthesis graphene for academic and industrial research at a reduced cost.

Acknowledgement

The HOD Chemistry, Nile University of Nigeria, Abuja, Prof. Sherali and Mr. Muhammad Baba Ari, Lab. assistant are being acknowledged for the synthesis of graphene.

References

1. Nwoke, M. A. U., Uwadiale, G. G. O. O., Kollere, M. A. (1997). Flotation of low-grade Birnin Gwari and Alawa graphite, Nigeria. Mining, Metallurgy & Exploration, 14(2), 54-56.
2. RMRDC graphite location chart www.rmrdc.gov.ng (accessed May, 5 2019).
3. Barma, S. D., Baskey, P. K., Rao, D. S., Sahu, S. N. (2019). Ultrasonic-assisted flotation for enhancing the recovery of flaky graphite from low-grade graphite ore. Ultrasonics Sonochemistry, 56, 386-396.

4. Jo G, Choe M, Lee S, Park W, Kahng Y.H and Le T. (2012). Nanotechnology 23, 112001.
5. Geim, A.K. Novoselov, K.S. (2007). The Rise of Graphene. Nature Materials, 6, 183-191.
6. Paulchamy B, Arthi G, Lignesh BD. (2015). A Simple Approach to Stepwise Synthesis of GO Nanomaterial. J Nanomed Nanotechnology 6, 253.
7. Coros, Maria., Pogacean, Florina, Pruneanu, Stela. (2020). Green synthesis, characterization and potential application of rGO. Physica E: LD Systems and Nanostructures, 113971.
8. Brodie, B.C. (1859). On the Atomic Weight of Graphite. Philosophical Transactions of the Royal Society of London, 149, 249-259.
9. Staudenmaier L., (1898) Verfahren zur darstellung der graphits aure, Ber. Dtsch. Chem. Ges. 31(2), 1481.
10. Hummers W.S, and Offeman R.E. (1958). Preparation of GO, J. Am. Chem. Soc. 80(6), 1339.
11. Marcano, D.C, Dmitry V. Kosynkin, Jacob M. Berlin, James M. Tour (2010) Improved Synthesis of Graphene Oxide, ACS Nano, 4(8).
12. Novoselov, K. S. (2004). Electric Field Effect in Atomically Thin Carbon Films, 306(5696), 666-669.
13. Wan, F., Qiu, X., Chen, H., Liu, Y., Xie, H., Shi, J., … Zhou, C. (2018). Accelerated electron extraction and improved UV stability of TiO2 based PSCs by SnO2 based surface passivation. Organic Electronics, 59, 184-189.
14. Chimonyo, W., Fletcher, B., Peng, Y. (2020). The differential depression of an oxidized starch on the flotation of chalcopyrite and graphite. Minerals Engineering, 146, 106114.
15. Pallab B., Roberto F., and Hiroshi K. (2011). Comprehensive semiconductor science and technology, Reference Work, Elsevier Science, www.sciencedirect.com.
16. Zeng, F., Sun, Z., Sang, X., Diamond,Su, D. S. (2011). In situ one-step electrochemical preparation of graphene oxide nanosheet-modified electrodes for biosensors. ChemSusChem, 4(11), 1587-1591.
17. Yoo, D., Kim, J. and Kim, J.H. (2014). Direct Synthesis of Highly Conductive PEDOT: PSS/Graphene Composites and Their Applications in Energy Harvesting Systems. Nano Research, 7, 717-730.
18. Ramesh, P., Bhagyalakshmi, S., Sampath, S. (2004). Preparation and physicochemical and electrochemical characterization of exfoliated graphite oxide. Journal of colloid and interface science, 274(1), 95-102.
19. Zaaba, N.I., Foo, K.L., Hashim, U., Voon, C.H. (2017). Synthesis of Graphene Oxide using Modified Hummers Method: Solvent Influence. Procedia Engineering, 184(1), 469-477.
20. Hu, W., Yang, S., & Yang, S. (2019). Surface Mod. of TiO2 for PSCs. Trends in Chem.
21. Eluyemi, M. S., Eleruja, M. A., Ajayi, E. O. B. (2016). Synthesis and chx of graphene oxide and reduced graphene oxide thin films deposited by spray pyrolysis method. Graphene, 5(3), 143-154.
22. Loryuenyong V., B. Jindawattanawong, A. Buasri (2015) The Fabrication of TiO2-Tin Oxide/RGO Photoanodes for DSSC, Trans Tech Publications, Switzerland, 1662- 9795, 780, 32-36.
23. Roose, B., Sandeep P., Ullrich S., (2015) Doping of TiO2 for SSCs (Review) Chem. Soc. Rev., 44, 8326-8349.
24. Snaith H.J., L. Schmidt-Mende. (2007). Advances in Liquid-Electrolyte and Solid-State Dye-Sensitized Solar Cells, Adv. Mater., 19(20), 3187–3200.
25. Gagandeep, Singh, M., Kumar, R., Singh, V. (2020). Investigating the impact of layer properties on the performance of p-graphene/CH3NH3PbI3/n-csi solar cell using num. modelling. Sup and Mic, 106468.
26. Kim, F., Cote, L.J. Huang, J. (2010). Graphene Oxide: Surface Activity and Two-Dimensional Assembly. Advanced Materials, 22, 1954-1958.
27. Vijayalakshmi, R., Rajendran, V. (2012). Syn and char. of nano-TiO2 via diff methods. A.A.S. Res, 4(2), 1183-1190.
28. Wali, Q., Elumalai, N. K., Iqbal, Y., Uddin, A., & Jose, R. (2018). TPSCs. Ren. and Sust Energy Reviews, 84, 89-110.
29. Petersen, C. L., Hansen, T. M., Bøggild, P., Boisen, A., Hansen, O., Grey, F. (2002). Scanning microscopic four-point conductivity probes. Sensors and Actuators A: Physical, 96(1), 53-58.
30. Li, J. C., Wang, Y., & Ba, D. C. (2012). Characterization of semiconductor surface conductivity by using microscopic four- point probe technique. Physics Procedia, 32, 347-355.
31. Hasegawa, S., Shiraki, I., Tanabe, F., Hobara, ... & Grey, F. (2003). Electrical conduction through surface superstructures measured by microscopic four-point probes. Surface Review and Letters, 10(06), 963-980.
32. Kazmi, S.A., S. Hameed, A.S. Ahmed, M. Arshad, & A. Azam. (2016) Electrical and optical properties of graphene –TiO2 nanocomposite and its applications in DSSC, Jnr of Alloys and Compounds, 691, 659-665.
33. Snaith, H. J. (2013). Perovskites: the emergence of a new era for low-cost, high-eff SCs, J. Phys. Che.Lett. 4, 3623-3630.
34. Alam, S.N., Sharma, N. Kumar, L. (2017). Synthesis of Graphene Oxide by Modified Hu mmers Method and Its Thermal Reduction to Obtain RGO. Graphene, 6, 1-18.
35. Patil, M. R., Shivakumar, K. S., Rudramuniyappa, M. V., Rao, R. B. (2000). Flotation studies on graphite ores of shivaganga area, Madurai district, Tamilnadu. Journal of Metallurgy and Materials Science, 42(4), 233-241.
36. Acharya, B. C., Rao, D. S., Prakash, S., Reddy, P. S. R., …. & Biswal, S. K. (1996). Processing of low-grade graphite ores of Orissa, India. Minerals Engineering, 9(11), 1165-1169.
37. Becerril, H. A., Mao, J., Liu, Z., Stoltenberg, R. M., Bao, Z., …… & Chen, Y. (2008). Evaluation of solution-processed reduced graphene oxide films as transparent conductors. ACS nano, 2(3), 463-470.
38. Kremer F, and Schonhals A, (2003). Broadband Dielectric Spectroscopy Springer, Berlin.
39. Acharya BC, Rao DS, Prakash S, Reddy PSR, Biswal SK. (1996). Pro. of low-grade graphite ores of Orissa, India. Minerals Engineering. 1996. 9(11):1165-1169.